Fizika Nizkikh Temperatur, 2008, v. 34, No. 7, p. 645–652

Creep and depinning of vortices in nontwinned $YBa_2Cu_3O_{6.87}$ single crystal

A.V. Bondarenko, A.A. Zavgorodniy, D.A. Lotnik,
M.A. Obolenskii, and R.V. Vovk

Department of Low Temperature Physics, V.N. Karazin Kharkiv National University,
4 Svoboda sq., Kharkiv 61077, Ukraine
E-mail: Aleksandr.V.Bondarenko@univer.kharkov.ua

Y. Biletskiy

Department of Electrical and Computer Engineering, University of New Brunswick, 15 Dineen drive,
Fredericton, New Brunswick, E3B5A3, Canada

Received February 25, 2008

We present the results of transport study of vortex dynamics in $YBa_2Cu_3O_{6.87}$ crystals in the magnetic field **H**||**c**. In low magnetic fields, $H < 4$ kOe, the measurements were performed in the range of vortex velocities $\nu = 10^{-4}$–2 m/s, which covers thermal creep and flux flow modes. The pinning force F_p nonmonotonically depends on magnetic field in both modes, though low-field minimum in the $F_p(H)$ curve shifts to higher fields with increased velocity ν, that is interpreted as partial ordering the vortex lattice. The increase of the pinning force F_p upon increasing the field, which is observed in the flux flow mode in fields $H \geq 3$ kOe, is interpreted by presence of finite transverse barriers. The barriers result in preserving the entangled vortex solid phase for the above-barrier vortex motion along the action of the Lorentz force. We also show that field variation of the depinning current has a single maximum, while field variation of the pinning force inside deep creep mode has two maxima. Appearance of two maxima is associated with nonmonotonous field variation of the activation energy $U_{\rm pl}$, which corresponds to plastic vortex creep mediated by motion of the dislocations.

PACS: 74.25.Qt Vortex lattices, flux pinning, flux creep;
74.72.Bk Y-based cuprates.

Keywords: superconductivity, vortices, phase transitions, dynamics, single crystals.

Nonmonotonous field variation of the pinning force $F_p(H)$, which is observed in the low-T_c ($NbSe_2$ [1–3], MoGe [3], and V_3Si [4]), middle-T_c (MgB_2 [5,6]), and high-T_c (BiSrCaCuO [7], YBaCuO [8,9]) superconductors, is a subject of long-time interest. Several models were proposed to explain this phenomenon. Increase of the pinning force with magnetic field can be explained by softening of the elastic moduli near the upper critical field [1] or near the melting line [10] that causes better accommodation of vortices to the pinning landscape. In frames of the collective pinning theory [11] the nonmonotonous $F_p(H)$ dependence inside the thermal creep regime is explained by competition between decrease of the depinning current J_d and increase of the activation energy with increased field [12]. Two alternative explanations [13,14] predict transformation of an ordered vortex solid (VS) phase, which forms in low fields and is characterized by a decrease of the force F_p with increased field, to a disordered VS phase, which forms in high fields and is characterized by increase of the force F_p with the field. These models are supported by correlation between the field H_{OD} corresponded to an ordering in the VS structure [15] and onset of the F_p increase [7] in BiCaSrCuO crystals. It should be noted that the «Lindemann criteria model» [13] predicts gradual transition from the topologically ordered VS to topologically disordered VS, which imply gradual crossover from the decreased to increased branch of the $F_p(H)$ dependence. In contrast, the quantitative theory proposed in Ref. 14 predicts real phase transition from the vortex-lattice state to the vortex-glass state, which is accompanied by sharp increase in the depinning current. Therefore these two models can be dis-

tinguished through different field variation of the current J_d at the order-disorder (OD) transition.

An actual problem of the VS phase is the nature of its ordering under an increased vortex velocity v. It was proposed [16] that transverse vortex displacements u_t induced by the quenched disorder reduce with increased velocity, $u_t \propto 1/v$; and the increase of the velocity above some critical value v_c results in a dynamic transition from the disordered to ordered state. It was later justified [17] that the increase in v leads to a suppression of the pinning in the longitudinal (with respect to **v**) direction only, while pinning barriers remain finite in the transverse direction. This leads to formation of longitudinal static channels for vortex motion, which were experimentally observed in $NbSe_2$ single crystals [18]. Finite transverse barriers and formation of longitudinal static channels were also observed in numerical simulations of the moving VS [19]. Numerical simulations [20–22] allow to determine correlation between the pinning force by individual defect f_p, the velocity v, and ordering of the VS phase with increased driving force, $F_L = JB/c$. For the situation of strong pinning force f_p it was found that disordered VS phase persists even at the over-barrier vortex motion, which realizes at transport currents $J > J_d$. In this case one can expect increase of the pinning force with the field at large vortex velocities.

Increase of the force F_p with the field at slow and high speeds of vortex motion was experimentally observed in low-T_c superconductors, such as $NbSe_2$ [1,2] and V_3Si [4], and in middle-T_c superconductor MgB_2 [6]. However, in these superconductors increase in the pinning force realizes in high magnetic fields, $h \equiv H / H_{c2} \geq 0.7$, and in close vicinity to the melting line $H_M(T)$. Therefore this increase can be associated both with the OD transition and softening of elastic moduli close to the $H_{c2}(T)$ or $H_M(T)$ lines. The aim of this work is experimental study of pinning and dynamics of VS phase in $YBa_2Cu_3O_{7-\delta}$ superconductor when increase of the pinning force with the field realizes well below the $H_{c2}(T)$ and $H_M(T)$ lines.

The measurements were performed on detwinned $YBa_2Cu_3O_{7-\delta}$ crystal, annealed in an oxygen atmosphere at 500°C for one week. Such anneal corresponded to an oxygen deficiency $\delta \approx 0.13$ [23], and $T_c \approx 91.8$ K with $\Delta T_c = 0.3$ K. The crystal then was held at room temperature for 7 days. As seen in Fig. 1, this caused reduction in the resistance and increase in the critical temperature. These changes agree with hypothesis that anneal of the $YBa_2Cu_3O_{7-\delta}$ crystals at room temperature leads to formation of clusters of oxygen vacancies [8]. This hypothesis implies a decrease of concentration of the oxygen vacancies in main volume of the crystal, and thus causes a decrease of the resistance R. Also, considering a bell-shaped $T_c(\delta)$ dependence with the maximum occurrence at $\delta \approx 6.92$ [24], the value of T_c in main volume of the crystal

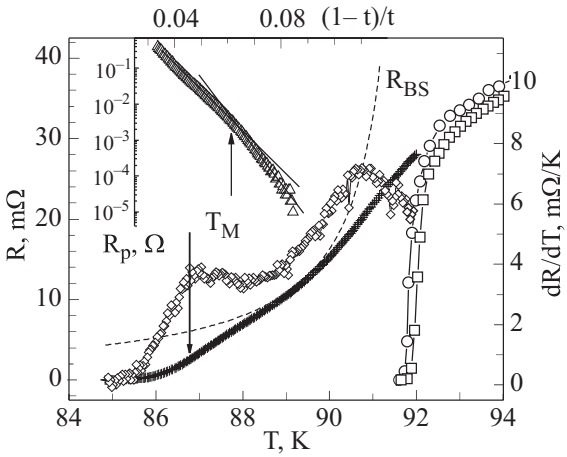

Fig. 1. The temperature variation of the resistance of just annealed in oxygen atmosphere crystal (circles) and after «anneal» of the crystal at room temperature for 7 days (squires), which were measured in zero field. Daggers and diamonds present respectively the $R(T)$ and $dR(T)/dT$ curves measured in a field of 15 kOe in the crystal, which was «annealed» at room temperature. Dashed line shows the $R_{BS}(T)$ dependence. The inset shows the $R_p(T)$ dependence (see the text), plotted in the $\log R_p$ vs $(1-t)/t$ scale.

increases due to decrease of the effective value of the δ. Thus one can expect that in investigated sample the point-like pinning potential, constituted by the isolated oxygen vacancies, coexists with the volumetric pinning potential, constituted by the clusters of oxygen vacancies. The investigated sample had rectangular shape with smooth surfaces; its dimensions were $3.5 \times 0.4 \times 0.02$ mm with the smallest dimension along the c axis; the current was applied along the largest dimension; and the distance between the current and potential contacts, and between the potential contacts was about 0.5 mm. The field variation of the pinning force was studied through measurement of the current-voltage characteristics, $E(J)$, using the standard four-probe method with dc current. The measurements were performed at a temperature of 86.7 K in the field **H**||**c**.

Figures 2,*a* and 2,*b* show results of measurements in magnetic fields up to 4 kOe, which are presented as the current variation of the vortex velocity $v = cE(J)/B$. Figure 2,*c* shows the current variation of the dynamic resistance $\rho_d = [dE(J)/dJ]/\rho_{BS}$ normalized by the flux flow resistance $\rho_{BS} = \rho_N B/B_{c2}$ [25]. At small currents the velocity and resistance exponentially increases with the current, and the value of ρ_d is much smaller than one. These peculiarities corresponds to the thermally activated flux motion. At high currents the velocity linearly increases with the current and the value of the resistance ρ_d is about one, indicating realization of the flux flow motion. Thus experimental data allow to determine field variation of the pinning force both inside the creep and flow regimes. The pinning force inside the creep regime can be characterized by the current J_v de-

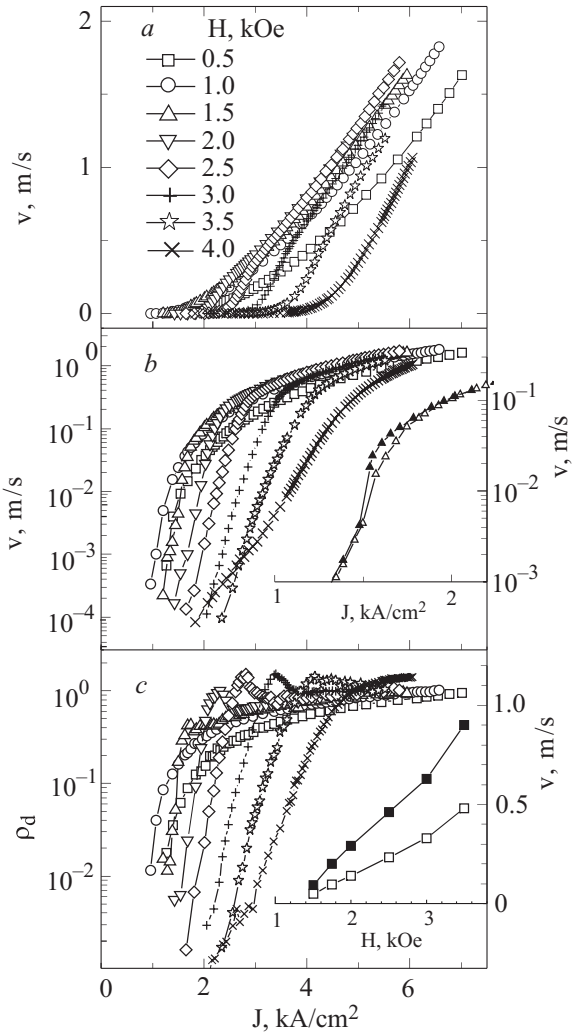

Fig. 2. The current variation of the vortex velocity v plotted in the linear (*a*) and semilogarithmical (*b*) scale, and current variation of the normalized dynamic resistance $\rho_d = [dE(J)/dJ]/\rho_{BS}$ plotted in the semilogarithmical scale (*c*). The inset of panel (*b*) shows the hysteresis effect in the $v(J)$ curve measured with the increased (light symbols) and decreased (dark symbols) current in a field of 1.5 kOe. The inset of panel (*c*) shows the field variation of the velocities v_p (light symbols) and $v_{\min}$ (dark symbols), which correspond to the peak and minimum position in the $\rho_d(J)$ curves, respectively.

termined at slow and fast vortex motion, which correspond to the creep and flow regimes. Experimental data allow also to determine the depinning current J_d by extrapolating linear parts of the $v(J)$ curves correspondent to the flux flow regime to zero velocity.

As one can see in Fig. 3, the currents J_d and J_v nonmonotonous vary with the field: in small magnetic field they decrease with increased field, while in high fields they increase with the field. First of all we note that minimum in the $J_v(H)$ and $J_d(H)$ dependence is observed in magnetic field much smaller compared to the upper critical field $H_{c2}(86.7\ \mathrm{K}) \approx 50$ kOe and the melting field $H_M(86.7\,\mathrm{K}) \approx 15$ kOe. Therefore increase of the

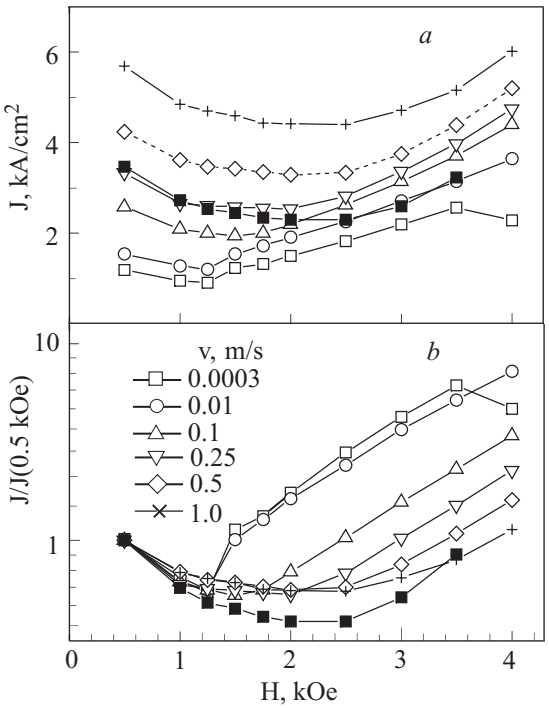

Fig. 3. (*a*) The field variation of the currents J_v, which correspond to different velocity criteria indicated in the panel (*b*). (*b*) The field variation of the currents J_v normalized by their values in a field of 0.5 kOe. The dark squares show the field variation of the current J_d.

currents J_d and J_v can not be attributed to softening of the elastic moduli of the vortex lattice. Nonmonotonous field variation of the current J_d contradicts to the collective pinning theory [11], which predicts monotonous decrease of this current with increased field. Also, gradual increase of the current J_d contradicts with the quantitative theory of Rosenstain and Zuravlev [14], which predicts a jump-like increase of this currents at the OD transition. Therefore we can assume that increase in the pinning force is associated with gradual transition from the ordered to disordered VS phase as it was proposed by Ertas and Nelson [13]. Different position of minima in the $J_v(H)$ and $J_d(H)$ curves is probably caused by the dynamic ordering of the VS phase [16,17]. Let us discuss field variation of the currents J_v and J_d in frames of the static [13] and dynamic [16,17] OD transitions in detail.

In frames of the Lindemann criteria model [13] the static OD transition occurs when transverse displacements of the vortex lines u_t induced by interaction of vortices with quenched disorder exceed the value of $c_L a_0$, where $a_0 \approx \sqrt{\Phi_0/B}$ is the intervortex distance, Φ_0 is the flux quantum, and c_L is the Lindemann number. The displacements $u_t = c_L a_0$ causes increase in the elastic energy $E_{\mathrm{el}} \approx c_L^2 \varepsilon \varepsilon_0 a_0$ [13,26], where ε is the anisotropy parameter, $\varepsilon_0 = (\Phi_0/4\pi\lambda)^2$ is the line energy, and λ is the field penetration depth. In low fields the energy E_{el} exceeds the pinning energy E_p. Therefore the ordered VS phase is formed, and this phase does not contain the topo-

logical defects. The pinning force of the ordered VS decreases with increased field due to inhancement of vortex–vortex interaction that makes pure accommodation of vortices to the pinning landscape. However the energy $E_{\rm el} \propto 1/\sqrt{B}$ reduces with increased field faster compared to the pinning energy, and therefore in high fields the energy $E_{\rm el}$ becomes smaller than E_p leading to transition of the ordered VS to the disordered one. The disordered VS contains dislocations, the screw components of which lead to entanglement of vortex lines. Therefore the increase in the pinning force at the OD transition can be cased by crossover from the 1D pinning of the ordered VS to 3D pinning of the disordered VS [13,27,28], and by better adaptation of the disordered phases to the pinning landscape [29,30].

Estimations presented below show that static OD transition in our sample is caused by vortex interaction with the clusters of oxygen vacancies rather than with the isolated oxygen vacancies. Indeed, for the point disorder the pinning energy is [11,13] $E_p \approx (\gamma\varepsilon^2\varepsilon_0\xi^4)^{1/3}(L_0/L_c)^{1/5}$, where $L_0 \approx 2\varepsilon a_0$ is the length of longitudinal fluctuations, $L_c \approx \varepsilon\xi(J_0/J_d)^{1/2}$ is the correlation length, $J_0 = 4c\varepsilon_0/(3\sqrt{3}\xi\Phi_0)$ is the depairing current, ξ is the coherence length, and $\gamma \approx (J_c\Phi_0/c)^2 L_c$ is the disorder parameter. Using realistic for the $YBa_2Cu_3O_{7-\delta}$ superconductor parameters ($\lambda = 500$ nm, $\xi = 4$ nm, and $\varepsilon = 1/7$) and experimental value of the depinning current $J_c < 5$ kA/cm^2 we obtain the energy $E_p < 2\cdot10^{-16}$ erg, which is about 25 times smaller compared to the elastic energy $E_{\rm el} \approx c_L^2\varepsilon\varepsilon_0 a_0 \approx 5\cdot10^{-15}$ erg estimated for the $c_L = 0.2$ and $H_{OD} = 1.25$ kOe. The pinning energy induced by vortex interaction with the clusters of oxygen vacancies equals the condensation energy $U_c \approx (H_c^2/8\pi)V_{\rm cl}$, where $H_c = \Phi_0/(2\sqrt{2}\pi\lambda\xi)$ is the thermodynamic critical field and $V_{\rm cl}$ is the volume of clusters. For spherical clusters with radius $r \approx \xi$ we obtain the energy $E_p \approx U_c \approx 10^{-14}$ erg, which is suitable for occurrence of the OD transition in the field of 1.25 kOe.

The minimum position in the $J_v(H)$ curves is not changed for the velocity criteria $v \le 10^{-2}$ m/s corresponded to the creep regime. This correlates with results of the magnetic measurements [8,9], which probe vortex creep at vortex velocities $v \approx 10^{-6}$ m/s [31]. From the point of view of the dynamic ordering this means that pinning energy is not changed inside the creep regime. Therefore the field $H_{OD} \approx 1.25$ kOe corresponds to the static OD transition, which is determined by the equality $E_{\rm el}(H_{OD}) = E_p(H_{OD})$, is not changed too. Increase of the velocity criteria above 10^{-2} m/s shifts the minimum position in the $J_v(H)$ curves towards higher fields that can be explained by *partial* dynamic ordering of the VS: the ordering makes pure adaptation of the vortex lines to the pinning landscape resulting in smaller value of the pinning force. It is important to note that in the flux flow regime the VS is the disordered phase that is manifested in an increase of the depinning current when magnetic field exceeds the value of 2.5 kOe. The disordered state of fast moving VS can be associated with persistence of the transverse pinning barriers, as it is predicted by the moving Bragg glass theory [17].

The pioneer work by Koshelev and Vinokur [16] assumes that suppression of pinning at high velocities v results in decrease of the amplitude $u_t \propto 1/v$. In frames of the Lindemann criteria model this leads to dynamic transition of the disordered VS to the odered VS when the velocity v exceeds the critical value v_c which corresponds to equality $u_t(v_c) = c_L a_0$. In contrast, persistence of the transverse barriers results in persistence of some part of the transverse displacements, the amplitude of which satisfy the Lindemann criteria, $u_{t,L} > c_L a_0$. This is evident from diagram presented in Fig. 4. This diagram shows the displacement $u_{t,L} = \sqrt{(u_\parallel)^2 + (u_\perp)^2}$ containing transverse $u_\perp$ (with respect to vector **v**) and parallel $u_\parallel$ component. In magnetic field **H**||**c** and in presence of the chaotic pinning potential spatial distribution of the displacements $u_{t,L}$ is isotropic. In the fields $H > H_{OD}$ the displacements $u_{t,L}$ are confined between the lower $u_{t,L}^{\rm low} = c_L a_0(H)$ and upper $u_{t,L}^{\rm up}$ boundaries, which are shown by the dashed and solid circles, respectively. It is easy to show that in frames of the cage potential model [26] the upper boundary is determined by relation $u_{t,L}^{\rm up} = c_L a_0(H_{OD})(H_{OD}/H)^{1/4}$. Density of the displacements $n_{t,L}$ (the number of vortex

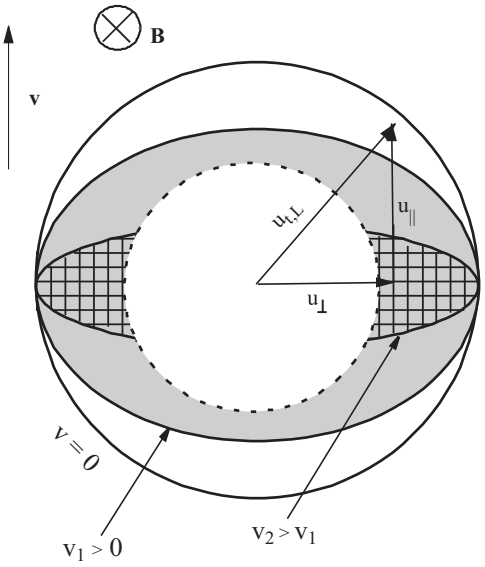

Fig. 4. Schematic presentation of the transverse displacement $u_{t,L}$, which satisfies the Lindemann criteria in magnetic field $H > H_{OD}$. The dashed and solid circles show the lower and upper boundaries of the displacements $u_{t,L}$ of the static VS. Two ellipsis's show evolution of the upper boundary with increase of vortex velocity v. The cross-hatched area corresponds to displacements $u_{t,L}$ of the fast moving VS.

displacements $u_{t,L}$ per unit length of vortex line) is proportional to the area of ring confined by the upper and lower boundary, and the density $u_{t,L}$ increases with the field because the upper boundary reduces with the field slowly compared to the lower boundary. Reduction of the component $u_{\parallel}$ with increased velocity v leads to reduction of the upper boundary in the longitudinal direction, as it is schematically shown by dotted ellipsis corresponding to vortex velocities $v_2 > v_1 \neq 0$. It is important to note, that for any finite velocity v the component $u_{\parallel}$ is finite, and thus the cross-hatched aria in the diagram (and therefore the density $n_{t,L}$) is also finite.

Considering that displacements $u_{t,L}$ produce the dislocations in the VS phase, and increase of the density $n_{t,L}$ results in an increase of the critical current [32], the field variation of the currents J_v and J_d can be explained in the following way. In low fields the ordered VS phase is formed. This phase does not contain dislocations and it is characterized by realization of the 1D pinning. Therefore the currents J_v and J_d decrease with increased field due to enhancement of the vortex–vortex interaction, making it difficult to fit the vortices in the pinning landscape. Above the OD transition the VS phase contains dislocations that results in realization of the 3D pinning [13], and therefore the current J_v, which corresponds to the creep regime, increases at the transition point H_{OD} due to dimensional crossover in the pinning [27,28]. Further increase of the current J_v with magnetic field is caused by increase of the density $n_{t,L}$, as it was found in Ref. 32. The density $n_{t,L}$ in the moving VS phase is smaller compared to that in the static VS, but it is finite and increases with the field. Therefore specific $J_d(H)$ dependence is determined by competition between decrease of the pinning force caused by enhancement of the vortex–vortex interaction and increase of the pinning force associated with increase of the density $n_{t,L}$. In our measurements the former mechanism dominates in magnetic fields $H \leq 2$ kOe, while the last one dominates in the fields $H \geq 3$ kOe.

Proposed interpretation agrees with numerical simulations of the moving 2D [19–21] and 3D [33] VS phases, which were performed for the case of strong pinning force f_p. First of all, it was shown that inside the flux flow regime the VS phase is the disordered one [19–21,33], and the transverse barriers remains finite [19]. Second, the $E(J)$ curves cross one another near the OD transition [33]. Third, our interpretation implies that cross-hatched area in the diagram collapses into a segment at $v \to \infty$, indicating that moving VS can be ordered at very large velocities v in agreement with conclusion of Ref. 33. Finely, the onset of VS ordering manifests itself as a peak in the $\rho_d(J)$ curves, and the end of ordering corresponds to value of the resistance $\rho_d(J) = 1$ [20,21]. In our measurements peak in the $\rho_d(J)$ curves appears in the fields $H > H_{OD}$, and above the peak position the resistance $\rho_d(J)$ drops down to the value of 1 in high fields, and it drops below the value of 1 in low fields. The last feature is probably associated with strong thermal creep in our measurements, which was not taken into account in the numerical simulations. Following numerical simulations, we determined the field variation of the velocities v_p and $v_{\min}$, which correspond to the peak and minimum position in the $\rho_d(J)$ curves, respectively. As seen in the inset of Fig. 2,*c*, the velocity $v_{\min}$ and the difference $\Delta v = v_{\min} - v_p$ increase with the field. This behavior is plausible considering that the lower boundary of the displacements $u_{t,L}$ decreases with the increased field that requires higher v's to decrease the amplitude below this boundary. Also, the difference between the upper and lower boundary of the displacements $u_{t,L}$, $\Delta u \approx$ $\approx c_L[a_0(H_{OD})(H_{OD}/H)^{1/4} - a_0(H)]$, increases with the field that results in increase of the difference Δv.

Our interpretation allows to explain occurrence of the hysteresis effect in the curve $v(J)$ measured with the increased and decreased current in a field of 1.5 kOe, see Fig. 2,*b*, and absence of the hysteresis effect below and well above the OD transition. Indeed, in close vicinity to the OD transition the density $u_{t,L}$ in the dynamic VS is reduced compared to that in the static VS by a factor $(H - H_{OD})/H_{OD} << 1$. Therefore small increase in the velocity v leads to the dynamic transition from the disordered to ordered state of the VS phase. In this case the «shaking temperature» model predicts the hysteresis effect, which reflects the «overheated state» of the ordered dynamic VS. Well above the OD transition decrease in density $u_{t,L}$ is not dramatic, and transition from strongly disordered static VS to less disordered dynamic VS occurs in a wide interval of velocities Δv without hysteresis. It is important to notice that the $E(J)$ curves measured after zero and nonzero field cooling coincide one with another indicating absence of metastable states in the VS. This agrees with experimental studies of the YBaCuO crystals: the metastable states exist in vicinity of the melting line, but they disappear far below this line [34].

Figure 5,*a* shows result of measurements in magnetic fields $H \geq 4$ kOe, which are presented in the scale $\rho(J)$ vs. $\sqrt{J}$, where $\rho(J) \equiv E(J)/J$. Figure 5,*b* shows current variation of the dynamic resistance $\rho_d = [dE(J)/dJ]/\rho_{BS}$. It is seen that inside the thermally activated creep regime (when the resistance ρ_d is musch smaller than one) current-voltage characteristics are described by equation

$$E(J) = \rho_0 J \exp\left[(-U_{\rm pl}/k_B T)\left(1 - \sqrt{J/J_{\rm pl}}\right)\right], \qquad (1)$$

which corresponds to plastic vortex creep mediated by motion of the dislocations [35,36]. In this equation ρ_0 is a constant, $U_{\rm pl}$ is the activation energy, and $J_{\rm pl}$ is the critical current which corresponds to the depinning of dislocations. The value of the current $J_{\rm pl}$ can be determined by extrapolation of the resistance ρ_d, correspondent to the

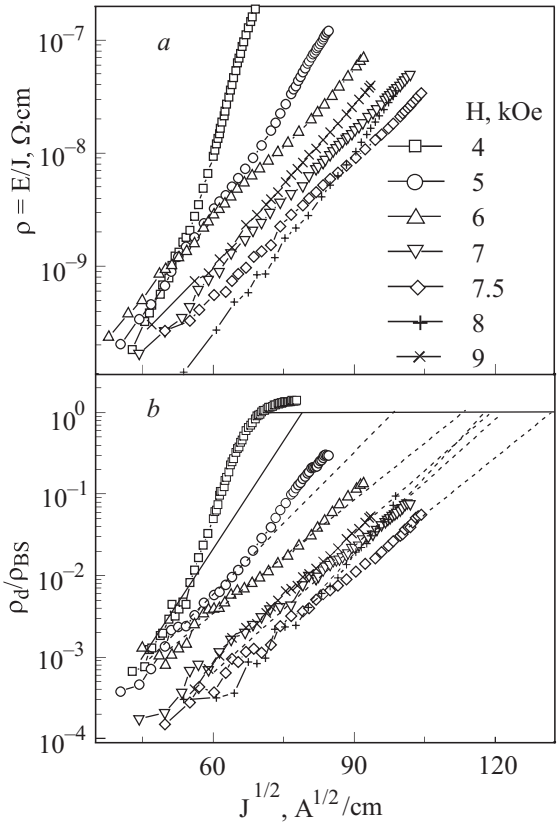

Fig. 5. The current variation of the resistance $\rho = E/L$ (*a*) and normalized dynamic resistance $\rho_d = [dE(J)/dJ]/\rho_{BS}$ (*b*) measured in different fields, which are indicated in the panel *a*.

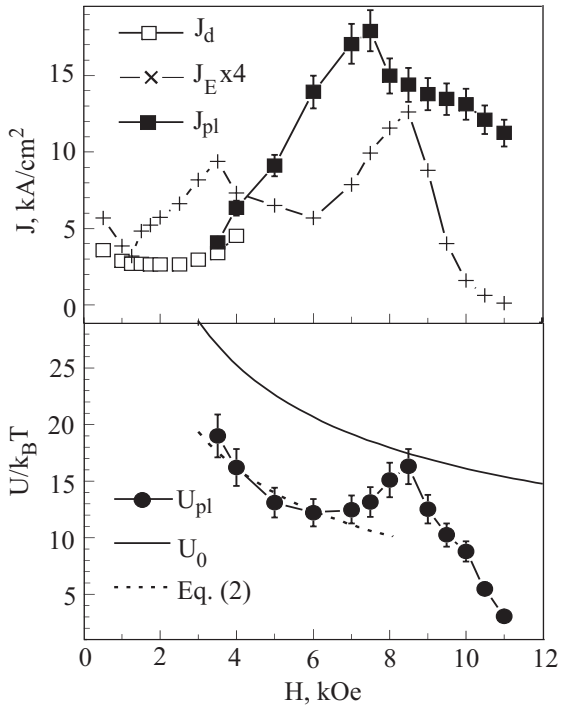

Fig. 6. (*a*) The field variation of the currents J_d, $J_{\rm pl}$, and J_E. (*b*) The field variation of the energies $U_{\rm pl}$ (circles) and U_0 (solid line). The dashed line presents $U_{\rm pl}(H)$ curve corresponded to Eq. (2) with the amplitude u_t described in the text.

creep regime, to one [32], as it is shown by the dashed lines in Fig. 4,*b*. Substituting this values of the current $J_{\rm pl}$ in Eq. (1), and fitting the experimental data corresponding to the creep regime by this equation, we obtained the value of energy $U_{\rm pl}$. Field variations of the currents J_d and $J_{\rm pl}$, and of the energy $U_{\rm pl}$ are shown in Figs. 6,*a* and 6,*b*, respectively. It is seen that the current $J_{\rm pl}$ is larger than the current J_d in contrast to their equality in twinned crystal [32]. This difference is reasonable considering that the disordered state of the VS in twinned crystal is caused by transverse deformations of the vortex lines $u_{t,TB}$ near the twin boundary planes, and that for vortex motion along the twinned planes the density of these deformations is not changed with increased velocity *v*. This means that VS's disorder in the twinned samples is not changed with increased velocity *v* and thus both the quasistatic and dynamic VS are characterized by the same depinning current. In our measurements the density $n_{t,L}$ decreases with increased velocity and therefore the VS undergoes partial ordering with increased velocity *v*. Therefore the current $J_{\rm pl}$, which characterizes strongly disordered quasistatic VS, is higher compared to the current J_d, which characterizes less disordered dynamic VS.

Comparison of the $J_{\rm pl}(H)$ and $U_{\rm pl}(H)$ dependencies shows that increase in the energy $U_{\rm pl}$, which is realized in the interval of the fields $6\,{\rm kOe} \le H \le 8.5\,{\rm kOe}$, is accompanied by crossover from the increased to decreased branch in the $J_{\rm pl}(H)$ dependence. The crossover indicates poorer adaptation of vortex lines to the pinning landscape. This leads to a decrease in the amplitude u_t, and therefore to an increase in the energy [37]

$$U_{\rm pl}(t,H) \approx U_0(t,H)(1-u_t/a_0)\,, \qquad (2)$$

where factor in the brackets comes from decrease of the effective intervortex distance $a_{\rm eff} \approx a_0 - u_t$. Here $t = T/T_c$ is the reduced temperature, and the energy $U_0(t,H) = 4\varepsilon\varepsilon_0 a_0 \propto (1-t)$ corresponds to displacements of the vortex fragments over intervortex distance a_0 [38]. The energy U_0 can be estimated from measurements of the $R(T)$ dependence in a magnetic field, using additional formula [11] $R(t) = [1/R_{BS}(t) - 1/R_p(t)]^{-1}$. Here the resistance $R_p(t)$ associates with vortex interaction with the chaotic pinning potential, and it exponentially decreases with the temperature [39,40],

$$R_p(t) = R_0 \exp[-U_0(t,H)/t]\,. \qquad (3)$$

Temperature variation of the resistance R and R_{BS}, and of the derivative dR/dT, which were measured in a field of 15 kOe, are shown in Fig. 1. Peak in the derivative dR/dT corresponds to the melting point [40], and in our measurements the melting temperature is $T_M(15\,{\rm kOe}) \approx 86.7$ K. The inset of Fig. 1 shows the dependence $R_p(t)$ presented in the scale $\ln R_p$ versus $(1-t)/t$, which takes into account temperature variation of the energy $U_0 \propto (1-t)$. At the

melting point a kink in the $R_p(t)$ dependence is observed, and below this kink temperature variation of the resistance R_p characterizes the VS phase. Fitting this part of the $R_p(t)$ dependence by Eq. (3) we obtained the energy $U_0(86.7\ \text{K}) = 13k_BT$ which corresponds to the magnetic field of 15 kOe. Field variation of the energy $U_0(H) = U_0(15\,\text{kOe})[a_0(H)/a_0(15\ \text{kOe})]$ is shown in Fig. 5,*b* by the solid line. In magnetic fields $H \le 6$ kOe the energy U_{pl} is about 1.6 times smaller than U_0. Fitting of the experimental data by Eq. (2) with the amplitude $u_t = u_{t,L}^{\text{upper}} \approx c_L a_0(H_{OD})[H_{OD}/H]^{1/4}$, which is shown by the dashed curve in Fig. 6,*b*, gives reasonable value of the Lindemann number $c_L \approx 0.25$. Therefore gradual increase of the energy U_{pl}, which is observed in the interval of magnetic fields $6\,\text{kOe} \le H \le 8.5$ kOe, and equality of the energies U_{pl} and U_0 at $H = 8.5$ kOe really indicate that the amplitude u_t gradually decreases due to worsening adaptation of vortices to the pinning landscape. This can be caused by increase of the vortex–vortex interaction, by change in the ratio of the vortex lines density and density of the clusters of oxygen vacancies, and by increased effect of the thermal fluctuations near the melting point of the VS phase. Justification of contribution of each of these mechanisms requires additional experimental studies. In particular it is desirable to study evolution of the $J_{\text{pl}}(H)$ and $U_{\text{pl}}(H)$ dependencies with the temperature, with the oxygen concentration, and with the «annealing» time of samples at room temperature.

Figure 6,*a* shows field variation of the current J_E determined at an electric field criterion of $E = 1$ μV/cm, which is close to the resolution level in our measurements, $E = 0.3$ μV/cm. It is seen that the current J_E has two peaks at $H = 3.5$ and 8.5 kOe. The current J_E is an analog of the «critical» current J_m determined in the magnetization measurements [31], though magnetization measurements probe vortex creep at smaller electric field, $E < 10$ nV/cm. Two peaks in the $J_m(H)$ dependence were previously observed in both low-T_c and high-T_c [41] superconductors, and their nature is still unresolved problem. Our measurements show that the depinning current has only one peak at $H = 7.5$ kOe. Appearance of two peaks in the $J_E(H)$ dependence is caused by nonmonotonous field variation of the activation energy U_{pl}. The first peak (at $H = 3.5$ kOe) is a result of competition between increase of the depinning current and decrease of the activation energy with increased field, while the second peak is a result of competition between decrease of the depinning current and increase of the activation energy with increased field. In both cases the field variation of the activation energy is dominant deep inside the creep regime, and therefore in magnetic fields $H \ge 3.5$ kOe the field variation of the current J_E is analogous to the field variation of the activation energy U_{pl}.

In conclusion, we have investigated pinning and dynamics of vortices in $YBa_2Cu_3O_{6.87}$ crystal in the magnetic field **H**||**c**. The measurements allowed to elucidate two aspects of pinning and dynamics of the vortex solid phase. One of them is the nature of static and dynamic order–disorder transition. We show that the static OD transition in our sample is caused by vortex interaction with the clusters of oxygen rather than with the isolated oxygen vacancies, and this transition leads to increase of the pinning inside the creep regime. Increase of the vortex velocity shifts the minimum position in the $F_p(H)$ curves towards higher fields that is caused by *partial* dynamic ordering of the VS, which makes pure adaptation of the vortex lines to the pinning landscape. Therefore field variation of the pinning force of the fast moving VS phase is determined by competition between decrease of the pinning force associated with enhancement of the vortex–vortex interaction and increase of the pinning force associated with the increased disorder of the VS phase. The increase of the pinning force within the flux flow mode, which is observed in fields $H \ge 3$ kOe, is interpreted by presence of finite transverse barriers. The barriers result in preserving the entangled vortex solid phase for the above-barrier vortex motion along the action of the Lorentz force. Another aspect of pinning and dynamics of the vortex solid phase, which was elucidated in our measurements, is appearance of two peaks in the field variation of the pinning force deep inside the creep regime. We show that both peaks are associated with nonmonotonous field variation of the activation energy U_{pl} corresponded to the plastic vortex creep mediated by motion of the dislocations.

The authors dedicate this work to the 80th anniversary of A.M. Kosevich whose works in the field of physics of real crystals were reflected in the field of vortex solid state containing dislocations.

1. S. Bhattacharya and M.J. Higgins, *Phys. Rev. Lett.* **70**, 2617 (1993); M.J. Higgins and S. Bhattacharya, *Physica* **C257**, 232 (1996).
2. Y. Paltiel, E. Zeldov, Y. Myasoedov, M.L. Rappaport, G. Jung, S. Bhattacharya, M.J. Higgins, Z.L. Xiao, E.Y. Andrei, P.L. Gammel, and D.J. Bishop, *Phys. Rev. Lett.* **85**, 3712 (2000).
3. N. Kokubo, T. Asada, K. Kadowaki, K. Takita, T.G. Sorop, and P.H. Kes, *Phys. Rev*. **B75**, 184512 (2007).
4. A.A. Gapud, D.K. Christen, J.R. Thompson, and M. Yethiraj, *Phys. Rev*. **B67**, 104516 (2003).
5. M. Pissas, S. Lee, A. Yamamoto, and S. Tajima, *Phys. Rev. Lett*. **89**, 097002 (2002).
6. H.J. Kim, H.S. Lee, B. Kang, P. Chowdhury, K.H. Kim, and S.I. Lee, *Phys. Rev*. **B70**, 132501 (2004); *ibid*. **B71**, 174516 (2005).
7. B. Khaikovich, E. Zeldov, D. Majer, T.W. Li, P.H. Kes, and M. Konczykowski, *Phys. Rev. Lett*. **76**, 2555 (1996).

8. H. Kupfer, Th. Wolf, C. Lessing, A.A. Zhukov, X. Langon, R. Meier-Hirmer, W. Schauer, and H. Wuhl, *Phys. Rev*. **B58**, 2886 (1998).
9. M. Pissas, E. Moraitakis, G. Kallias, and A. Bondarenko, *Phys. Rev*. **B62**, 1446 (2000).
10. W.K. Kwok, J.A. Fendrich, C.J. van der Beek, and G.W. Crabtree, *Phys. Rev. Lett*. **73**, 2614 (1994).
11. G. Blatter, M.V. Feigel'man, V.B. Geshkenbein, A.I. Larkin, and V.M. Vinokur, *Rev. Mod. Phys*. **66**, 1125 (1994).
12. L. Krusin-Elbaum, L. Civale, V.M. Vinokur, and F. Holtzberg, *Phys. Rev. Lett*. **69**, 2280 (1992).
13. D. Ertas and D.R. Nelson, *Physica* **C272**, 79 (1997).
14. B. Rosenstein and V. Zhuravlev, *Phys. Rev*. **B76**, 014507 (2007).
15. R. Cubbit, E.M. Forgan, G. Yang, S.L. Lee, D. Paul, H.A. Mook, M. Yethiraj, P.H. Kes, T.W. Li, A.A. Menovsky, Z. Tarnavski, and K. Mortensen, *Nature* (London) **365**, 407 (1993).
16. A. Koshelev and V. Vinokur, *Phys. Rev. Lett*. **73**, 3580 (1994).
17. T. Giamarchi and P. Le Dossal, *Phys. Rev. Lett*. **76**, 3408 (1996).
18. M. Marchevsky, J. Aarts, H.P. Kes, and M.V. Idenbom, *Phys. Rev. Lett*. **78**, 531 (1997); F. Pardo, F. de la Cruz, P.L. Gammel, E. Bucher, and D.J. Bishop, *Nature* (London) **396**, 348 (1998).
19. K. Moon, R.T. Scalettar, and G.T. Zimanyi, *Phys. Rev. Lett*. **77**, 2778 (1996); C.J. Olson and C. Reichhardt, *Phys. Rev*. **B61**, R3811 (2000).
20. M.C. Faleski, M.C. Marchetti, and A.A. Middleton, *Phys. Rev*. **B54**, 12427 (1996).
21. A.B. Kolton, D. Dominguez, and N. Grobech-Jensen, *Phys. Rev. Lett*. **83**, 3061 (1999).
22. H. Fangor, P.A.J. de Groot, and S.J. Cox, *Phys. Rev*. **B63**, 064501 (2001).
23. P. Schleger, W.N. Hardy, and B.X. Yang, *Physica* **C176**, 261 (1991).
24. R. Liang, D.A. Bonn, and W.N. Hardy, *Physica* **C304**, 105 (1998).
25. J. Bardeen and M.J. Stephen, *Phys. Rev*. **140**, 197 (1965).
26. V. Vinokur, B. Khaikovich, E. Zeldov, M. Konczykowski, R.A. Doyle, and P.H. Kes, *Physica* **C295**, 209 (1998).
27. R. Wordenweber and P.H. Kes, *Phys. Rev*. **B34**, 494 (1986).
28. E.H. Brandt, *Phys. Rev*. **B34**, 6514 (1986).
29. M.J.P. Gingras and D.A. Huse, *Phys. Rev*. **B53**, 15193 (1996).
30. T. Giamarchi and P. Le Doussal, *Phys. Rev.* **B55**, 6577 (1997).
31. H. Kupfer, A. Will, R. Meier-Hirmer, Th. Wolf, and A.A. Zhukov, *Phys. Rev*. **B63**, 214521 (2001).
32. A.V. Bondarenko, Yu.T. Petrusenko, A.A. Zavgorodniy, M.A. Obolenskii, and V.I. Beletskii, *to be published*.
33. A. van Otterlo, R.T. Scalettar, G. Zimanyi, R. Olsson, A. Petrean, W. Kwok, and V. Vinokur, *Phys. Rev. Lett*. **84**, 2493 (2000).
34. J.A. Fendrich, U. Welp, W.K. Kwok, A.E. Koshelev, G.W. Crabtree, and B.W. Veal, *Phys. Rev. Lett*. **77**, 2073 (1996).
35. W.K. Kwok, J.A. Fendrich, V.M. Vinokur, A.E. Koshelev, and G.W. Crabtree, *Phys. Rev. Lett*. **76**, 4809 (1996).
36. J.P. Hirth and J. Lothe, *Theory of Dislocations*, Chap 15, John Wiley & Sons, New York (1982).
37. A.V. Bondarenko, A.A. Prodan, Yu.T. Petrusenko, V.N. Borisenko, F. Dworzchak, and U. Dedek, *Phys. Rev*. **B64**, 092513 (2001).
38. A.V. Bondarenko, A.A. Prodan, M.A. Obolenskii, R.V. Vovk, and T.R. Arouri, *Fiz. Nizk. Temp*. **27**, 463 (2001) [*Low Temp. Phys*. **27**, 339 (2001)].
39. V.M. Vinokur, V.B. Geshkenbein, A.I. Larkin, and M.V. Feigel'man, *Z. Eksp. Teor. Fiz*. **100**, 1104 (1991) [*Sov. Phys. JETP* **73**, 610 (1991)].
40. J.A. Fendrich, W.K. Kwok, J. Giapintzakis, C.J. van der Beek, V.M. Vinokur, S. Flesher, U. Welp, H.K. Viswanathan, and G.W. Crabtree, *Phys. Rev. Lett*. **74**, 1110 (1995).
41. S. Sakar, D. Pal, P.L. Paulose, S. Ramakrishnan, A.K. Grover, C.V. Tomy, D. Dasgupta, Bimal K. Sarma, G. Balakrishnan, and D. McK. Paul, *Phys. Rev*. **B64**, 144510 (2001), and references therein.